Applied Physics A (2019) 125:124
https://doi.org/10.1007/s00339-019-2413-3

Applied Physics A
Materials Science & Processing

REVIEW

A review on the numerical modeling of CdS/CZTS-based solar cells

Assiya Haddout[1] · Abderrahim Raidou[1] · Mounir Fahoume[1]

Received: 27 November 2018 / Accepted: 14 January 2019

Abstract
CZTS thin-film is now one of the most promising materials for the sustainable absorption of solar cells. Recently, there has been interest in enhancing efficiency and reducing costs of manufacturing CZTS-based solar cells. Nevertheless, there is no report focused on explaining the role of numerical modeling's help to understand this cell. In this review, we discuss the advantages and the challenges of the experimental pure sulfide CZTS-based solar cells. The softwares used in simulations thin-films solar cells are discussed. The solutions for improving efficiency of CdS/CZTS-based solar cells using numerical modeling are also discussed.

1 Introduction

Photovoltaic solar power generation has been growing exponentially in recent decades. The technology based on the deposition of thin layers represents a technological challenge in which many researchers have focused its attention on the mastery of this technology as it allows manufacturing devices at lower cost while maintaining the basic physical properties required for good performance. Among the thin films, those based on copper, indium, gallium and selenium [Cu (In, Ga) Se_2: CIGS] and those based on cadmium telluride (CdTe) offer higher conversion efficiencies about 22% [1]. However, the toxicity of cadmium and the low abundance of indium and tellurium are the main drawbacks of energy production. Nowadays, some semiconductor materials are derived from the CIGS chalcopyrite structure by replacing the rare elements In and Ga with less expensive elements such as Zn and Sn, respectively, while the derived structure is CZTS [2]. Pure sulfide Cu_2ZnSnS_4 (copper zinc tin sulfide or CZTS), has kesterite structure, and it is an absorbing layer for the solar cell, with a direct band gap (1.4–2.0 eV) and high absorption coefficient (~ 10^5 cm^{-1}), according to the Table 1. Many publications were published during the years with the aim of improving the efficiency of CZTS solar cell (Fig. 1). Nevertheless, this cell has not yet reached a higher efficiency of 22% [1] for CIGS and CdTe thin-film solar cells.

However, the pure sulfide CZTS-based thin-film solar cell has an efficiency of 11% [19] achieved in 2018, later, achieved 9% [20] in 2016.

To find an explanation for this low performance, a complete understanding is necessary. The aim is to reduce a number of real tests and costs in short time. It is necessary to have methods that give manufactures additional ideas on how to vary their production processes to improve the output performance of the solar cells. Therefore, the model is an approximation close to the real system. Solar cell modeling always offer an easy way to understand the effect of microscopic phenomena on device macroscopic parameters. Numerous publications were published in these last years with the aim of improving efficiency of CZTS solar cells using simulation (Fig. 2).

The objective of our article is a review where we will focus on all the software used for the simulation of pure sulfide CZTS-based solar cell and the results obtained on the efficiency using simulation optimization. First of all these steps, it is important to explain what are the challenges limiting the increased cell performances of the CZTS solar cell.

✉ Assiya Haddout
assiyahd@gmail.com

Abderrahim Raidou
a.raidou@yahoo.fr

Mounir Fahoume
mfahoume@yahoo.fr

[1] Condensed Matter Physics Laboratory, Department of Physics, Ibn Tofail University, B.P 133, 14000 Kenitra, Morocco

Published online: 23 January 2019

Table 1 Evolution of electrical properties of pure sulfide CZTS thin-film per year

Year	Band gap (eV)	Absorption coefficient (cm^{-1})	p-Carrier concentration (cm^{-3})	References
1997	1.45	10^4	–	[3]
2001	1.4–1.45	10^4	–	[4]
2005	1.5	10^4	8×10^{18}	[5]
2006	1.51	10^4	4.5×10^{17} to 8.2×10^{18}	[6]
2007	1.5	10^4	–	[7]
2008	1.49	–	1×10^{16}	[8]
2009	1.43	–	3.3×10^{18}	[9]
2010	1.49–1.5	10^4	3.1×10^{20}	[10]
2011	1.51	3×10^4–4×10^4	–	[11]
2012	1.5	–	10^{18}	[12]
2013	1.6–1.67	10^4	–	[13]
2014	~1.4	~10^4	~10^{17}	[14]
2015	1.46–1.68	10^5	–	[15]
2016	1.38–2.0	–	6.1×10^{17}–9.4×10^{19}	[16]
2017	2.0	–	7×10^{18}	[17]
2018	1.6–1.9	–	1.5×10^{19}–3.6×10^{19}	[18]

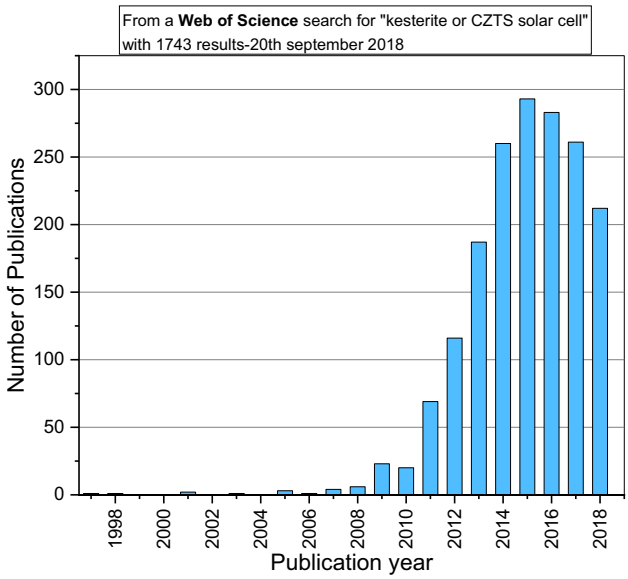

Fig. 1 Evolution of the number of publications per year for CZTS material till September 2018; source: Web of Science database

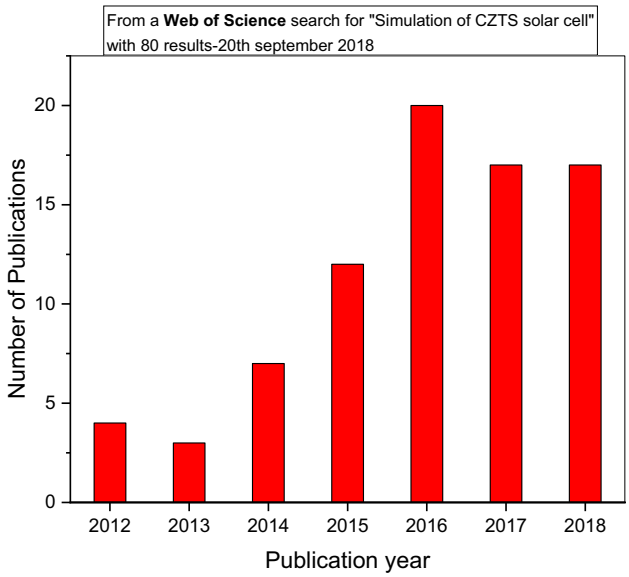

Fig. 2 Evolution of the number of publications per year for simulation of CZTS solar cell till September 2018; source: Web of Science database

2 Difficulty in enhancing CdS/CZTS-based solar cell efficiency: experimental

A CZTS solar cell has a low efficiency, which is an essential challenge. Table 2 and Fig. 3 present the output performances of CdS/CZTS-based thin-film solar cells from the literature per year.

It is remarked from these results (Fig. 3) obtained from the general figure of all CdS/CZTS-based structures that the efficiency still remains unchanged during this 21-year period and that it has increased only with 10.35%.

The performance parameters of various CZTS-based solar cells reported in literature [19, 26–32, 34–37] have been compiled to ascertain their performance compared to theoretical Shockley–Queisser (SQ) [41] limit and these are shown in Fig. 4, and the cell performances (J_{SC}, V_{OC}, FF, and η) varying with the band gap of CZTS films from 1.45 to 1.62 eV. It can be noted that there is a significant deficit of the experimentally observed performance

Table 2 Output performance of the experimentally stated CdS/CZTS-based solar cell from the literature

Year	η (%)	J_{SC} (mA/cm^2)	V_{OC} (mV)	FF (%)	References
1997	0.66	6.0	400.0	27.7	[3]
2001	2.62	14.11	522.4	35.54	[21]
2003	5.45	–	–	60.0	[22]
2005	4.53	12.53	629.0	58.0	[23]
2007	1.74	6.78	546.0	48.4	[24]
2008	6.77	17.9	610.0	62.0	[25]
2009	3.4	14.8	563.0	41.0	[26]
2010	6.81	17.8	587.0	65.0	[27]
2011	2.03	9.69	575.0	36.4	[28]
	2.23	10.2	529.0	41.6	[29]
	4.59	15.44	545.0	54.57	[30]
	8.4	19.5	661	65.8	[31]
2012	7.3	22	567	58.10	[32]
2013	7.6	20.14	–	–	[33]
	5.75	20.5	593	48	[34]
2014	6.2	19	603	55	[35]
	8	17.7	719	62.8	[36]
2015	6.6	22.0	567.4	52.8	[37]
2016	7.1	21.8	614.3	55.5	[38]
	9.4	21.3	700.0	63.0	[39]
2017	6.63	33.1	517.7	38.6	[40]
2018	**11.01**	**21.74**	**730.6**	**69.27**	[19]

Table 3 Output performance of the experimentally stated CZTS and CIGS solar cell from the literature

Structure	η (%)	J_{SC} (mA/cm^2)	V_{OC} (mV)	FF (%)	References
CIGS	17.0	33.6	674	75.5	[42]
	22.6	37.8	741	80.6	[43]
CZTS	4.28	22.25	507	38.0	[44]
	7.23	19.2	636	58.7	[45]

parameters compared to the SQ limit (solid lines in Fig. 4). To be more precise, we compared the output performance of CZTS solar cells with CIGS solar cells (Table 3).

The comparison of output performances of CZTS and CIGS shows, that there is a large gap between these two solar cells' results. To enhance CZTS efficiency, it is important to examine factors affecting the output performance, such as J_{SC}, V_{OC}, and FF that can be used to improve the efficiency of CZTS cells. Various researches have been carried out to investigate where these problematic areas exist. To achieve the high-efficiency CZTS such as CIGS cells, a more detailed understanding of the nature of defects in the absorber layer (CZTS) as well as the intra- and interlayer interfaces must be achieved. The first fabrication of pure sulfide CZTS solar cell is with structure GLS/Mo/CZTS/CdS/ZnO:Al/Al (Fig. 5). Where Mo is a back contact coated on GLS substrate with 1 µm of thickness [25], CZTS is absorber layer with 0.5–2.2 µm of thickness [3, 25, 37], CdS buffer layer with 20–70nm [3, 25] of thickness and ZnO:Al window layer with 0.6µm [3].

This conventional structure has a variety of issues affecting the performances of the CZTS photovoltaic cell, according to the literature. Figure 6 presents the regions contributing to the lower performance which is:

1. *CdS buffer layer* Its n–type layer plays an important role in the fabrication of solar cell. However, it has characteristics which affect the environment and the performance of the solar cell, they are: (1) this material provokes important environmental damage caused as a result of the large quantity of cadmium-containing waste resulting from the deposition process and (2) its band gap energy of about 2.4–2.5 eV [46] restricting the optimal performance of the solar cell. This performance gap can principally be caused by the large open circuit voltage (V_{OC}) deficit($E_g/q - V_{OC}$, E_g is the bandgap, q is the electron charge) [47]. In addition, its low bandgap causes significant optical absorption losses and thus reduces the short-circuit current density of the solar cell. According to experimental study it is possible to replace CdS with an environment-friendly buffer layer and also enhanced the performances cell. Alternative buffer layers proposed by the literature are: ZnO [48, 49], ZnS [50, 51], In_2S_3 [52, 53], Zn(O,S) [54], $Zn_{1-x}Sn_xO_y$ [55, 56] and ZnSnO [57].
2. *CZTS absorber layer* Many issues in CZTS absorber layer contribute to larger V_{OC} deficiency and small J_{SC}, which are:

   (a) *Secondary phases* The precipitate secondary phases in the CZTS-thin films include ZnS, Cu_xS, SnS_x, and Cu_2SnS_3 etc. On account of their intrinsic properties, the detrimental effects of secondary phases on CZTS devices are different (see Table 4) [58]. The formation of secondary phases with a band gap smaller than the band gap of the absorber leads to a larger V_{OC} deficiency as they introduce electronic states within the band gap of the absorber which can act as traps and recombination centres. This increases the rate of recombination, lowering the V_{OC}. On the other hand, the formation of secondary phases with a band gap larger than the band of the absorber narrows the conduction pathways for charge carrier transport, increasing R_S and lowering the FF of the solar cell [59]. As a remedy, etchants have been used to remove these unwanted secondary phases after they are formed (see Table 4) [58]. However, some of these secondary phases in CZTS play important roles in its optical properties. Mamedov et al. [60]

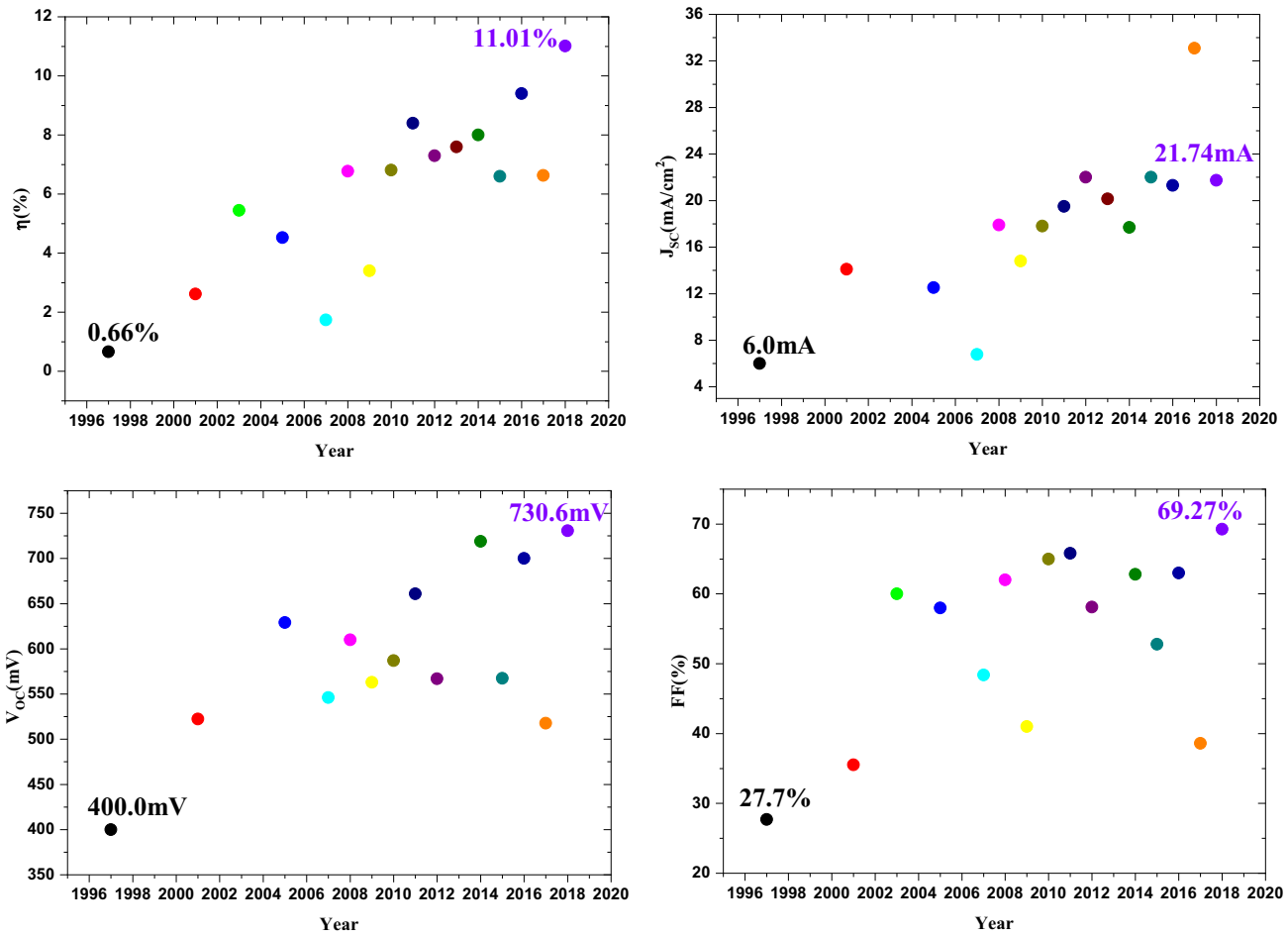

Fig. 3 Evolution of output performances of CdS/CZTS -based solar cells from literature per year

demonstrated using the theory of effective mass that Cu_2S caused a reduction in the band gap and improved light absorption by the CZTS at all photon energies of sunlight, while the SnS changed the optical properties of the CZTS only at large photon energies beyond the solar spectrum.

(b) *Band gap tailing* Gokmen et al. [61] suggested that band gap tailing may be a cause for the larger V_{OC} deficiency found in CZTS solar cells .Band gap reduction can lead to a smaller activation energy for recombination, because the presence of a high density of tail states reduces the effective band gap of the semiconductor. Consequently, the V_{OC} that can be produced in CZTS-based solar cells is limited [59]. Band tailing caused by a large amount of Cu/Zn antisite. Silver alloying may be a promising method for dealing with this issue. As Ag tome is much larger than that of Cu or Zn, if Cu can be partially substituted by Ag, the Cu/Zn antisite number will be suppressed which decreases the band tailing problem and corresponding non-radiative recombination. Yan et al. [62] found Ag incorporation for CZTS exerts many positive influences, one of these effects is it increases band gap.

(c) *Grain boundaries* (*GB*) Their presence in CZTS-based absorbers is detrimental to the efficiency of the solar cell due to the structural defects associated with grain boundaries, which causes recombination. Therefore, it is advantageous to minimize grain boundaries or to passivate the grain boundary defects [59]. It is well known that sodium at grain boundaries (GBs) increases the photovoltaic efficiencies of CZTS. Liu et al. [63] present the mechanism about how the Na enhances the photovoltaic performance of CZTS through passivating the GB defect states.

(d) *High density of charged defects* It worsens the extent of band-gap tailing, which, contributes to a larger VOC deficiency. In addition, it increases the probability of recombination and it is responsible for the small minority carrier lifetime in CZTS-

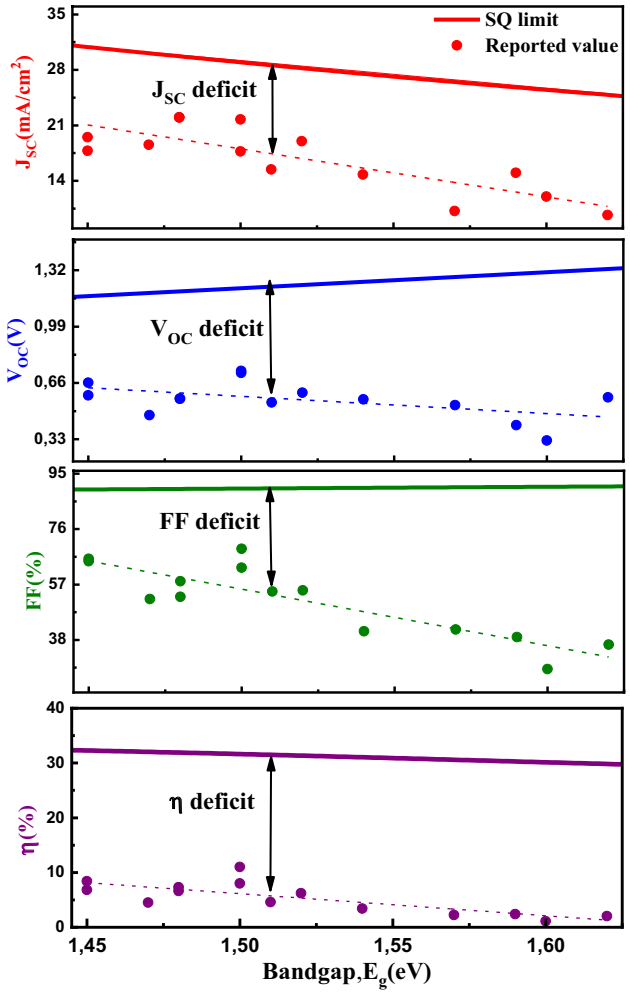

Fig. 4 Variation performance parameters of CZTS solar cell as a function of band gap, for laboratory solar cells reported in the literature (filled circles) [19, 26–32, 34–37], guide to eye for the variation with E_g (dashed line) and the corresponding SQ limit (solid line) [41]. The double-sided arrows mark the deficit in the observed solar cell parameters compared to the corresponding SQ limit

based solar cell. The minority carrier diffusion length Ld is dependent on the minority carrier lifetime [59]. L_d is an important parameter which is used to characterize quality of absorber material. It is well known that short L_d of the absorber negatively affects both J_{SC} and V_{OC}. The presence of defects and secondary phases reduces L_d which limits the thickness of CZTS absorber layer [64].

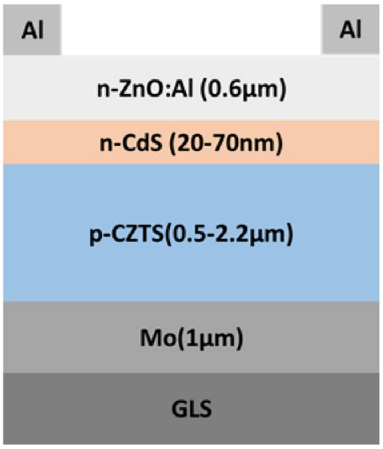

Fig. 5 Conventional structure of the CZTS solar cell

In the same context of the absorber layer, Courel et al. [65] insist to improve CZTS crystalline quality. Because they found CZTS films are characterized by low minority carrier diffusion length (L_d) values in the range of 100–171 nm. In the other study, Courel et al. [66] demonstrated CZTS-thin films processed under stoichiometric are responsible for lower solar cell performances. As a solution, they demonstrated CZTS deposited under optimal compositional ratios present better structural and morphological properties as well as lower contribution of secondary phases along with band gap energy values near to 1.5 eV as required for solar cell applications.

3. *CdS/CZTS interface* Suboptimal band alignment is the key problem of this interface. Indeed, the formation of a band alignment of the cliff conformation at the level of the CdS/CZTS region contributes to a higher V_{OC} deficit by reducing the potential difference that can be generated between the quasi-Firm levels of the p-CZTS layer and n-CdS layer under illumination systems. Using one of the alternative buffer materials listed in the part (1) as a solution to band alignment problems. In other studies, with an interest in the properties of the CdS buffer layer were

Table 4 Band gap of secondary phases with the method used to remove it [58]

Compound	Band gap	Potential detriment	Etchant
ZnS insulator	3.54–3.68	Insulating, reduce device-active area	HCl solution
Cu_xS ($1 \le x \le 2$) (p-type)	1.21–2.2	Metallic, shunted solar cell	KCN solution or H_2O_2 solution
SnS_x (x=1, p−type) (x=2, n−type)	1.11–2.6	Pull down the V_{OC} of the devices forms diode and barrier for carrier collection	$(NH_4)_2S$ solution
Cu_2SnS_3	0.98–1.35	Affect carrier collection efficiency	Br_2/MeOH

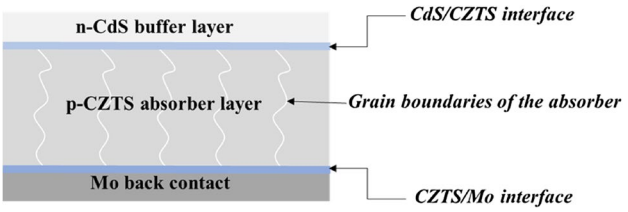

Fig. 6 Regions contributing to the lower performance of CZTS solar cells

solved this problem of large V_{OC} deficiency. Hong et al. [67] have observed that V_{OC} deficiency was improved as the thickness of the CdS buffer increased to 92 nm, then decreased with thicker CdS buffer layer. Rondiya et al. [68] have found the optical band gap ~ 1.5 eV for CZTS and ~ 2. 35 eV for CdS films. So the band of CdS/CZTS hetero-junction formation leads to spike-like CBO of ~ 0.55 eV which can improve the performance of the cell. In 2018, Yan et al. [19] found a new phase between CdS and CZTS is elemental inter-diffusion where a band alignment and high efficiency were achieved.

4. *CZTS/Mo interface* The Mo back contact is attributed to two main problems in kesterite solar cells: (1) decomposition reactions caused by instability of the Mo/CZTS interface and high sulphur pressure (S) required for the sulfidation process, resulting in too thick MoS_2 and defects at the back contact region; (2) a Schottky barrier presence at the Mo/CZTS interface eliminates hole transport and increases recombination at the back interface and that causes to increase the R_S of the solar cell and thereby reducing the FF of the solar cell. Various strategies are used for reducing the thickness of MoS_2 and therefore enhance the device performance by introducing an interfacial layer between Mo and the CZTS layer, such as TiB_2 [69], Ag coating, a thin ZnO coating on the Mo back contact [70], ZnO [71], Si_xN_y [72], MoO_3 [73], etc.

In summary, several factors have been suggested for this V_{OC} deficit, including a large number of charge defects associated with band tailing, co-existence of secondary phase unfavourable band alignment at the CZTS/CdS heterojunction interface and an undesirably thick MoS_2 layer at the rear of the CZTS cell. These problems cause high recombination at the bulk of the absorber and at interfaces, low minority carrier lifetime and high series resistance in CZTS solar cells, limiting the cell performance. To deal with these problems, alternative buffer layers, Ag incorporation, Na passivation of the Grain Boundaries, CZTS deposited under optimal compositional ratios, interfacial layer between Mo and the CZTS layer were used. The problem of short minority carrier diffusion length was not yet resolved. For that, a better understanding of CZTS solar cells for long-term stability, is required to help propel this relatively new technology forward.

The aim of this work is to reduce a number of real tests and costs in a short time. It is necessary to have methods that give manufacturers additional ideas on how to vary their production processes to improve the performance of the solar cell. Therefore, an approximation close to the real system which is the model, is required. The analysis of the characteristic curves of the CZTS thin-film solar cell leads to the hypothesis that these losses originate from causes contributing to the low performance included in the layers and interfaces previously defined. However, these models often can support the hypothesis, and provide a physical explanation of the mechanism behind the loss. In addition, they can predict the quantitative impact of changes in material properties on device performance and suggest ways to change the deposition process and improve performance.

For that purpose, we will review the kesterite solar cell numerical simulation in the following section. Numerical simulation is another choice after experience and theory. In this review, we will discuss if the simulation can find other solutions to improve the experimental efficiency of the CZTS solar cell, as well as reduce the time and the material losses, all of which with the hope of achieving optimal results.

Table 5 Software used for simulating solar cells

Software	Dimension	Link
PC1D	1D	https://www.pvlighthouse.com.au/cms/simulation-programs/pc1d
SCAPS	1D	http://scaps.elis.ugent.be/
AMPS	1D	http://www.ampsmodeling.org/
ADEPT	1D	https://nanohub.org/resources/adeptnpt
AFors-Het	1D	https://www.helmholtz-berlin.de/forschung/oe/ee/si-pv/projekte/asicsi/afors-het/index_en.html
ATLAS	2D/3D	https://www.silvaco.com/products/tcad/device_simulation/atlas/atlas.html
Sentaurus	1D/2D/3D	https://www.synopsys.com/silicon/tcad/device-simulation/sentaurus-device.html
COMSOL	1D/2D/3D	https://www.comsol.com/

Table 6 Critical issues for a thin-film PV simulation program [86]

Multiple layer
Band discontinuities in E_C and E_V: $\Delta E_C$and ΔE_V
Large band gap: E_g>2–3.7 eV
Graded band gap: $E_g(x)$ and also $\chi(x)$, $N_C(x)$, $N_V(x)$, $\alpha(x)$,…
Recombination and charge in deep bulk states
Simulation of non-routine measurements: J–V, C–V, C-f, QE(λ),…all as a function of T fast and easy to use

3 Numerical methods for solar cell device simulation

3.1 Numerical methods

We will start by the hypothesis of Dr. Siegfried Selberherr [74], "Modelling will become more and more important in the near future". This assumption is also supported by the fact that computer resources are going to be cheaper compared to drastically increasing costs for experimental investigations. Hence, many more engineers will have to face the problem of numerical device modeling to stay competitive. These assumptions have already been reached. Figure 2 made that the model has become more significant in recent years. Solar cell simulation has become increasingly used in recent years, and several calculation and simulation software packages have been developed by the research community in this field. Some of which are cited in Table 5.

The numerical modeling of solar cells can be divided into six main categories.

3.1.1 Fundamental physics

A several software programs have been created with a goal of modeling solar cells based on solving the basic semiconductor equations at the interfaces between the different layers of the structure. They have different possibilities and limitations, but the basic principal is the same. These equations are based on a drift–diffusion description of carrier transport, and they are three non-linear partial differential equations [75]:

$$\begin{aligned} \nabla \cdot D &= q(p - n + N), \\ \nabla \cdot J_{\mathrm{p}} &= q\left(G_p - R_{\mathrm{p}}\frac{\partial p}{\partial t}\right), \\ \nabla \cdot J_{\mathrm{n}} &= -q\left(G_{\mathrm{n}} - R_{\mathrm{n}}\frac{\partial n}{\partial t}\right), \end{aligned} \tag{1}$$

with the constitutive equations,

$$\begin{aligned} D &= -\varepsilon \nabla V, \\ J_{\mathrm{p}} &= -q\mu_{\mathrm{p}} p \nabla\left(V - V_{\mathrm{p}}\right) - kT\mu_{\mathrm{p}}\nabla p, \\ J_{\mathrm{n}} &= -q\mu_{\mathrm{n}} n \nabla\left(V + V_{\mathrm{n}}\right) + kT\mu_{\mathrm{n}}\nabla n, \end{aligned} \tag{2}$$

where, G_{p} and G_{n}, the generation rate terms; R_{p} and R_{n}, the recombination rate terms; N, the trapped charge concentration; $\varepsilon/\varepsilon_0$, the dielectric constant; μ_{p} and μ_{n}, the carrier motilities; and V_{p} and V_{n}, the band parameters.

3.1.2 Numerical methods

The Poisson and continuity equations are non-linear. For this reason, numerical methods are necessary to solve them, and by the discrete nature of these solving techniques, there is also a need to discretize the domains in which our equations are defined. In this section, we summarize the steps used to solve this semiconductor equation. The numerical methods vary between the simulators.

To start with, there is the discretization of differential equations either by the finite difference method generally used for 1D software such as AMPS [76] and AFORS-HET [77]. This method replaces differential operators with different operators. COMSOL Multiphysics [78] is multidimensional programming, which allows choosing between two methods: finite element method or finite volume method.

The non-linear algebraic system result by discretization on a mesh has been solved in an iterative method. The iterative method itself varies between programs as well. The numerical solving techniques or the iterative method used to solve non-linear equations for each program are as follows:

- PC1D [79] and ADEPT [75] use Newton Method;
- AMPS [76] and AFORS-HET [77] use Newton–Raphson method;
- SCAPS [80] uses a Gummel iteration scheme with Newton–Raphson substeps;
- ATLAS [81] uses Newton, Gummel, or Block methods.

3.1.3 Physical models

All simulation softwares are based essentially on these physical models:

Mobility In any software, the mobility of electrons and holes can either be set to fixed values throughout the region, or calculated based on the temperature and local carrier and doping density using one of the following models:

- Caughey and Thomas model (doping and temperature-dependent mobility) [82].
- Arora model (includes doping and temperature dependence) [83].
- Dorkel–Leturg model (includes dependence on temperature, doping, and carrier–carrier scattering) [84].
- Klaassen unified low-field mobility model (provides unified description of majority and minority carrier

mobility. In doing so, it includes the effects of lattice scattering, screened Coulomb charges, carrier–carrier scattering and impurity clustering effects at high concentrations) [85].

For example PC1D is based on the Caughey and Thomas model, and the Arora model.

Recombination There are three types of recombination for each layer in solar cell:

- Radiative (band-to-band) recombination (cm^3/s)
- Auger recombination (cm^6/s); it is divided in Hole Auger coefficient and Electron Auger coefficient
- Shockley–Read–Hall recombination; called also recombination at defects in SCAPS software.

There are other physical models which are very important for semiconductors and also used for solar cell simulation in any program that are: layer thickness (μm), refractive index ε, optical absorption coefficients α (cm^{-1}), permittivity, band gap E_g (eV), electron affinity χ (eV), CB (VB) effective density of stats N_C (N_V) (cm^{-3}) and donor (acceptor) density N_D (N_A) (cm^{-3}).

As well as some physics models are in a program and are not included in other programs, where we have:

- *Interface* SCAPS [80], AFORS-HET [77].
- *Tunneling* SCAPS [80],ATLAS [81].
- *Impact ionization* ATLAS [81].

3.1.4 Spatial dimensionality

In the solar cell simulation programs, the numbers of spatial dimensions used are as follows: one-dimensional (1D), two-dimensional (2D) and three-dimensional (3D). 1D simulation is generally acceptable for solar cells with conventional geometry, particularly for low-intensity solar cells and for semiconductor materials that are not well characterized. At high intensity, (2D) effects can be important even in conventional geometric solar cells and many high-efficiency cell designs require 2D or even 3D simulations. The interdigital back contact solar cell is an example of 2D geometry and the point contact solar cell is an example of 3D geometry by nature.

3.1.5 Device analysis

Simulation of the electrical characteristics of solar cells is the main objective of any device simulator. A typical solar cell is analysed under a specified solar spectrum and a spectral response. A powerful feature of numerical simulation is the ability to examine the spatial dependence of any internal model parameter, such as recombination and generation rates, electric field, current densities, carrier concentrations, etc. Such analyses will often help to understand the performance of the device.

3.1.6 User interface

This is the part that is necessarily the most dependent on the computer. A user-friendly interface is used to visualize all simulated quantities. All data (internal cell results and measurement methods) can be imported and exported and thus compared graphically. Heterostructures and some of its components (layers, interfaces) can be saved and loaded. The user can pre-select the measurement methods he or she wishes to use. Variations in arbitrary parameters can be made by selecting an arbitrary number of external and internal program input parameters to be modified with a specified range. As an output of a parameter variation, all possible internal cell results and measurements can be defined. Parameter variations can also be saved and reloaded.

In summary, Fig. 7 resumes the steps in the modelization of solar cells. Burgelman et al. [86] insisted on the ideal thin-film solar cell simulation program should, in addition, meet all the requirements listed in Table 6.

All programs use the Anderson model for calculating band discontinuities in E_C and E_V: $\Delta E_C = \Delta\chi$ and $\Delta E_V = \Delta\chi + \Delta E_g$. Table 7 compares some simulation programs 1D thin-film solar cells depending on the criteria of Table 6. PC1D originally developed for (poly)crystalline silicon cells the number of layers is rather limited, only five layers are allowed per device. It is not useful to use in modeling thin-film solar cells as it does not perfectly match all the criteria of Table 6.It is not useful to use in modeling thin-film solar cells, because, it does not perfectly match all the criteria of Table 6. It is probably used for CdTe/CdS-based solar cell [87] if the parameter of layers is not graded, but for CIGS-based solar cell, this number of layers is almost certainly too low. Therefore the same applies to CZTS-based solar cell.

Table 7 shows that the software is perfect for modeling thin-film solar cells. For example, SCAPS is more advantageous than the other programs for helping understand the solar cell in which all parameters can be graded. Where we used it in the last works for study CdTe [88] and CZTS [89] solar cells. The other programs also were used to simulate CdTe, CIGS, and CZTS solar cells. In the next section, we focus on the simulation of CZTS solar cell of these different softwares.

3.2 Numerical simulation of CZTS thin-films solar cells: results

The numerical simulation of solar cells is an important means of predicting the effect of different parameters on

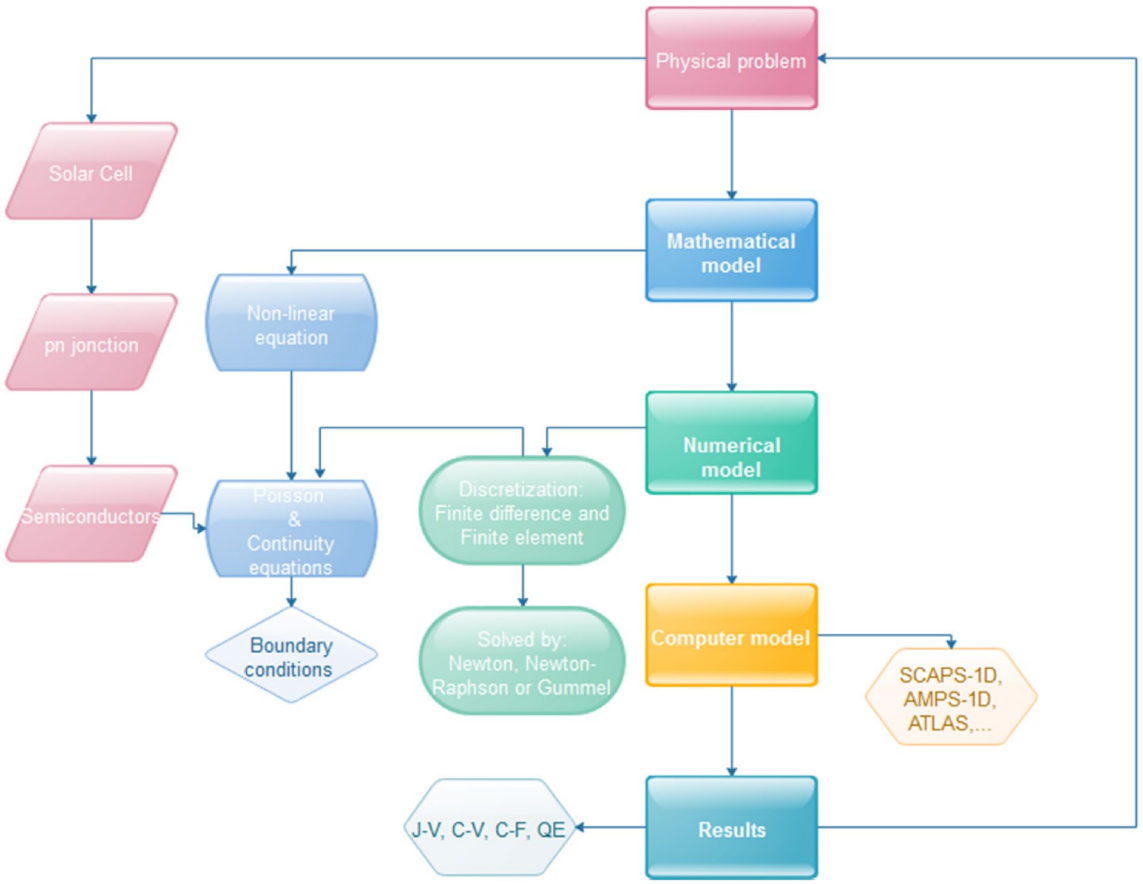

Fig. 7 Organigram resumes the steps in the modelization of solar cells

output performance and also examining the stability of the properties of structures and materials proposed. CdS/CZTS-based solar cells are naturally complex, with heterojunction structure. For this reason, it is necessary to use a numerical model with different dimensions. Two different approaches to study the performance of CZTS solar cells have been proposed numerically.

In the first method, it considers the fit of J–V and external quantum efficiency (EQE) curves as well as the dependence of solar cell parameters with temperature to extract information on device transport mechanisms and then to set possible paths to promote solar cell performance: Frisk et al. [90] based on their work on the reference device CZTS solar cell with 6.7% efficiency is used as input to a SCAPS device model. The results of the analysis of temperature-dependent current–voltage (J–V–T) demonstrate that the V_{OC} deficit observed in CZTS device is dominated by interface recombination. The absorption coefficient was modified after comparing data from reflectance–transmission (R–T) measurements with ellipsometry measurements, and calculations. The modified semi-empirical absorption coefficient permit to the extraction of the essential properties of the CZTS layer; diffusion length of 250 nm, CZTS band gap narrowing, shifting E_g to 1.35 eV, and interface defects. Increased the dimension from 1D to 2D for modeling CZTS solar cell is a way to capture the impact of lateral variations of, e.g. band gap fluctuations. Pu et al. [91] demonstrate that after constructing CZTS device model in 2D by using Sentaurus TCAD with use in the input the CZTS device reference with 6.9% of efficiency, they found the key underlying V_{OC} deficit is pinpointed to band gap fluctuation, which is backed by the simulation study on both QE tail and steady-state photoluminescence. The heterojunction interface recombination, together with disorder-induced band gap fluctuation contributed to 97% of V_{OC} loss. In summary, Frisk et al. [90] and Pu et al.'s [91] observations are consistent where it is depicted in Fig. 8, heterojunction interface recombination, and bulk disorder occupy 52.7% and 44.9% of V_{OC} loss, respectively, making other loss mechanisms seemingly negligible.

In the other method, it entails the calculation of device parameters, starting from some experimental inputs and assuming different transport mechanisms. In this case, the numerical model helps in understanding and predicting the effects of each region contributing to the lower performance cited in Fig. 6, where:

Table 7 Thin-film PV simulation program in 1D

	SCAPS [80]	AMPS [76]	AFors-Het [77]	ADEPT [75]
Multiple layer	7	30	–	–
Physics model	Interface Grading Generation Recombination: band-to-band; SRH and Auger Tunneling	Generation Recombination: band-to-band and SRH Schottky barrier	Recombination: band-to-band; SRH and Auger Interface modules: no interface or drift–diffusion or thermionic emission semiconductor/semiconductor heterojunction interface	Generation Recombination: band-to-band; SRH ;Auger; Defect State
Contacts	Front and back metal contacts: work function or flat-band	Front and back metal contacts	Metal/Semiconductor Schottky- or Schottky-Bardeen- or metal/insulator/semiconductor contact	Two charge neutral ohmic metal contacts
Measurements	Energy band; IV; AC; CV; CF; QE	Energy band; IV; QE	Energy band; IV; QE; PEL; SPV; QSS-PC; impedance IMP; CV; CT; TR and IV 2D	Energy band; IV; SR
Run under	Windows	Windows XP mode/Virtual PC	Windows	nanoHUB workspace, not yet to uses in Windows

1. *CdS buffer layer* Alternative buffer layers proposed by Zn(O,S) [92, 93]; ZnS [94]; ZnMgO [95]; etc…
2. *CZTS absorber layer* In this case, to improve the quality of this layer, several studies focus to optimize their physical properties. Patel and Ray [96] using SCAPS-1D, were enhancing the output performance of the CZTS solar cell by searching an optimum absorber thickness and acceptor concentration. Xu [97] was demonstrated using AFors-Het v2.4 program, the output performance of CZTS solar cell was improved using carrier concentration gradient of CZTS. Meher et al. [98] studied the effects of various CZTS layer parameters like thickness, carrier concentration, defect density, and mobility, on the cell performance using SCAPS. Adewoyin et al. [99] found using SCAPS, increase in absorption coefficient of the CZTS layer increased the short-circuit current (J_{SC}) while the optimization of the minority carrier lifetime further improved the open circuit voltage (V_{OC}). Khattak et al. [100] have optimized CZTS parameters such as the carrier concentration, thickness, and densities of absorber using SCAPS-1 D.
3. *CdS/CZTS interface* By numerical model many studies focus on conduction band offset (CBO) at CZTS/CdS junction. The interface is strongly dependent on the respective electron affinities (χ) which can be varied by changing the deposition conditions. The heterojunction interface can give rise to "spike"- (type-I) or "cliff"- (type-II) like CBO depending upon the difference in the electron affinities of the absorber and buffer layer. Using SCAPS-1D, Meher et al. [98] observe the transition from cliff- to spike-like behaviour in CB edge (under AM1.5G) with increase in χ_{CZTS} (Fig. 9a). The highest efficiency corresponding to a small spike of 0.1 eV for $\chi_{CZTS} = 4.3$ eV (Fig. 9b). Similar results were found by Kumar and Thakur [101], with a slightly positive CBO making a spike-type junction at the CZTS/CdS is advantageous for improving performance, and lowering the recombination current (Fig. 10).
4. *CZTS/Mo interface* Kumar and Thakur [101] have demonstrated the efficiency is enhanced by increasing back metal work function (ϕ_m) for $\phi_m \leq E_V$, but, for $\phi_m > E_V$ simulations do not converge. An alternative technique needs to be evolved for lowering the high work function added a BSF layer between CZTS/Mo. Zhao et al. [102] have demonstrated numerically using AMPS-1D that it is the true existence of the interface between CZTS/Mo that contributes to the low open circuit voltage (V_{OC}), and have verified the estimation of Wang et al. [103] which has found the existence of secondary phase, which consists of lower band gap phases such as Cu_2SnS_3 (~0.95 eV). Chelvanathan et al. [104] have studied the effects of p-MoS_2 and n-MoS_2 between CZTS/Mo (Fig. 11) by numerical analysis AMPS-1D.

Table 8 Summary of output performance of CZTS solar cells

Structure	η (%)	J_{SC} (mA/cm^2)	V_{OC} (V)	FF (%)	Comments
Mo/CZTS/CdS/AZO	6.77	17.9	0.61	62	Experiment [25]
Mo/CZTS/CdS/AZO	6.41	17.58	0.61	59.45	Modeled [89]
Pd/CZTS/CdS/AZO	12.26	18.73	0.97	67.32	Optimized [89]

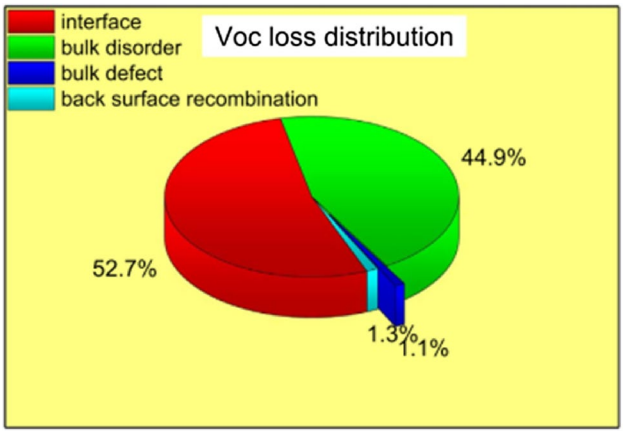

Fig. 8 Fraction of V_{OC} loss pertains to mechanisms including heterojunction interface, bulk disorder, bulk deep-level defects and back contact recombination parameterized into device model. The V_{OC} loss is calculated comparing to that of an ideal device without any loss mechanisms [91]

It is found out that p-MoS_2 layer in the CZTS solar cell induces the same adventitious effect as p-$MoSe_2$ in CIGS solar cell. However, n-MoS_2 layer forms ohmic contact with Mo which is detrimental as the recombination of electrons is likely to take place. Their results show that MoS_2 layer as thin as 50 nm is sufficient enough to induce adverse effect on the solar cell performance. This could be caused by the increase in series resistance of the solar cell as n-MoS_2 would inhibit hole current into Mo back contact due to the hole barrier between n-MoS_2 and Mo back contact. The increase in MoS_2 band gap and carrier concentration has also resulted in a detrimental effect on the performance cell mainly due to the possibility of electrons to drift towards the back contact and recombine. Adewoyin et al. [99] have demonstrated that the introduction of p-MoS_2 into the interface between the CZTS/Mo layers and the tuning of its band gap enhanced the open circuit voltage and using SCAPS-1D. Ferdaousa et al. [105] showed

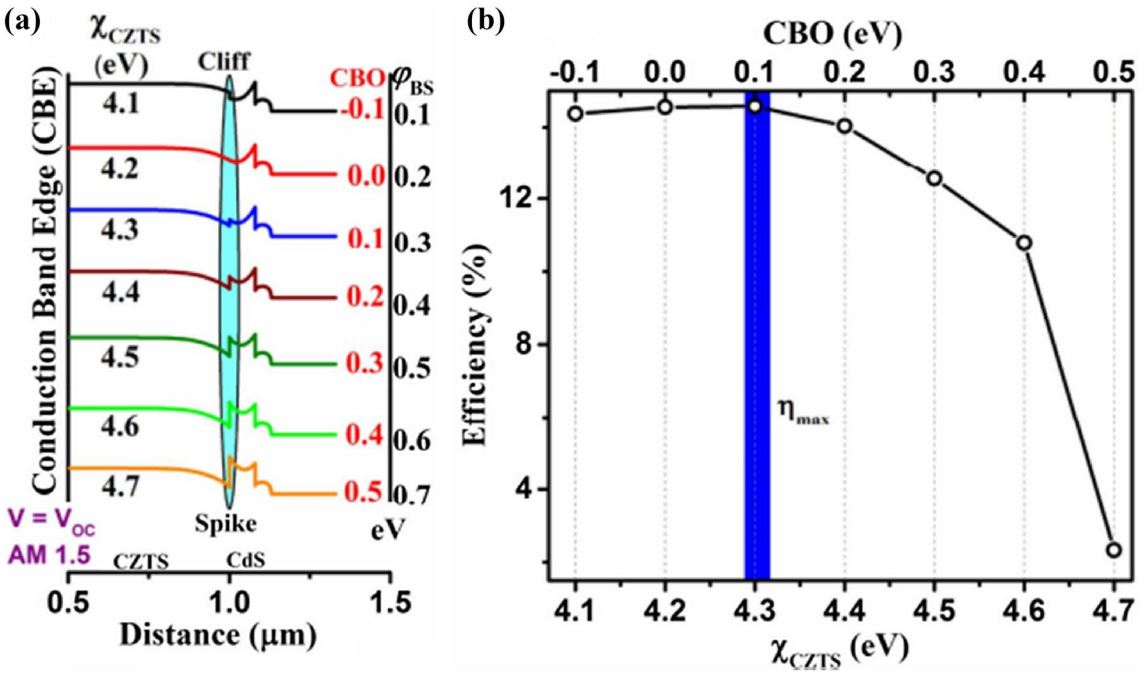

Fig. 9 **a** CBE for different values of χ_{CZTS} showing the cliff- to spike-like transition of CBO between CZTS/CdS junction, **b** solar cell efficiency as a function of χ_{CZTS} and CBO [98]

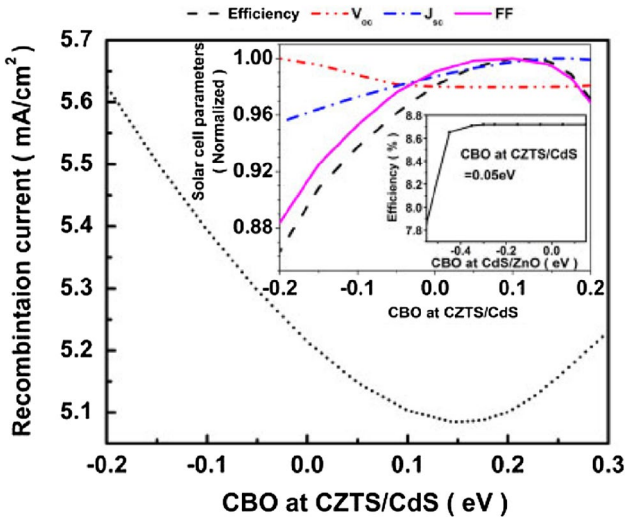

Fig. 10 Main panel: recombination current as a function of CBOCZTS/CdS. Inset: normalized performance parameters (V_{OC}, J_{sc}, FF, efficiency) as a function of CBOCZTS/CdS. Also shown in the inset is the variation of efficiency as a function of the conduction band offset at CdS/ZnO interface ($CBO_{CdS/ZnO}$) at a fixed value of $CBO_{CZTS/CdS}$ (=0.05 eV) [101]

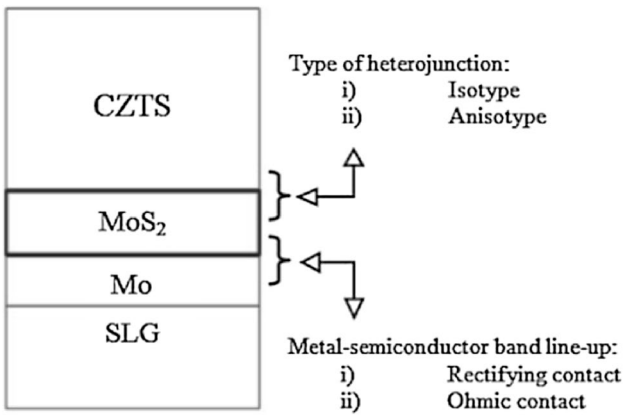

Fig. 11 Schematic of Mo/MoS_2/CZTS interfaces [104]

well the effects of both n and p-type MoS_2 on the overall CZTS solar cell's performance from the viewpoint of metal–semiconductor junction and heterojunction band alignment using wxAMPS-1D software. Generally, MoS_2 layer with lower electron affinity and band gap is preferred to induce desirable band alignment and subsequently result in higher efficiency. It was identified that the p-type MoS_2 with E_g of 1.2 eV and high carrier concentration of 10^{18} cm^{-3} can be beneficial for the CZTS solar cell in contrast to an n-type MoS_2 that can have an adverse effect on overall performance as a direct result of the n-p-n structure. This study shows the prospect of p-type MoS_2 as a beneficial back contact buffer layer. It also provides a limiting condition for n-MoS_2 if the formation of n-MoS_2 is absolutely unavoidable.

Some works have found a good agreement with experimental results and numerical results:

Haddout et al. [89] using SCAPS, the results of the simulation were in good agreement with reported experimental results [25] (Fig. 12a). For improving the model cell, they studied thickness and acceptor concentration effects of CZTS absorber layers, changing back contact and increased shunt resistance Fig. 12b and Table 8 summarizes the important results of this work (Fig. 13; Table 9).

Mopurisetty et al. [106] using Sentaurus, provide the results of model simulation which are in good agreement with reported experimental results [31].

In summary, we presented the two types of conventional structures of CZTS solar cells using different softwares in Table 10.

4 Conclusion

This article has focused on numerical simulation CZTS solar cell. A CZTS solar cell has a low efficiency, which is an essential challenge. An important deficit of the experimentally observed cell performances (J_{SC}, V_{OC}, FF and η) compared to the SQ limit and CIGS solar cells. The important regions of CZTS solar cells contributing to lower performance are: (1) CdS buffer layer; (2) CZTS absorbent layer; (3) CdS/CZTS interface and (4) CZTS/Mo interface. Due to the complex nature of the CZTS solar cell and the existence of many issues that limit output performance, a complete understanding is necessary. Therefore, an approximation close to the real system which is the model is required.

The numerical model is based on solving the basic semiconductor equations and help to understand and predict the effects of each region contributing to the lower performance using different software. Two different approaches to study the performance of CZTS solar cells have been proposed numerically. The first method, it considers the fit of J–V and external quantum efficiency curves as well as the dependence of solar cell parameters with temperature, where the reference device of CZTS solar cell was used as input in program to extract information on device transport mechanisms and then to set possible paths to promote solar cell performance. It was demonstrated that the heterojunction interface recombination, and the bulk disorder occupy 52.7% and 44.9% of V_{OC} loss, respectively, making other loss mechanisms seemingly negligible. In the other method, it entails the calculation of device parameters starting from some experimental inputs and assuming different transport mechanisms. In summary, the best solar

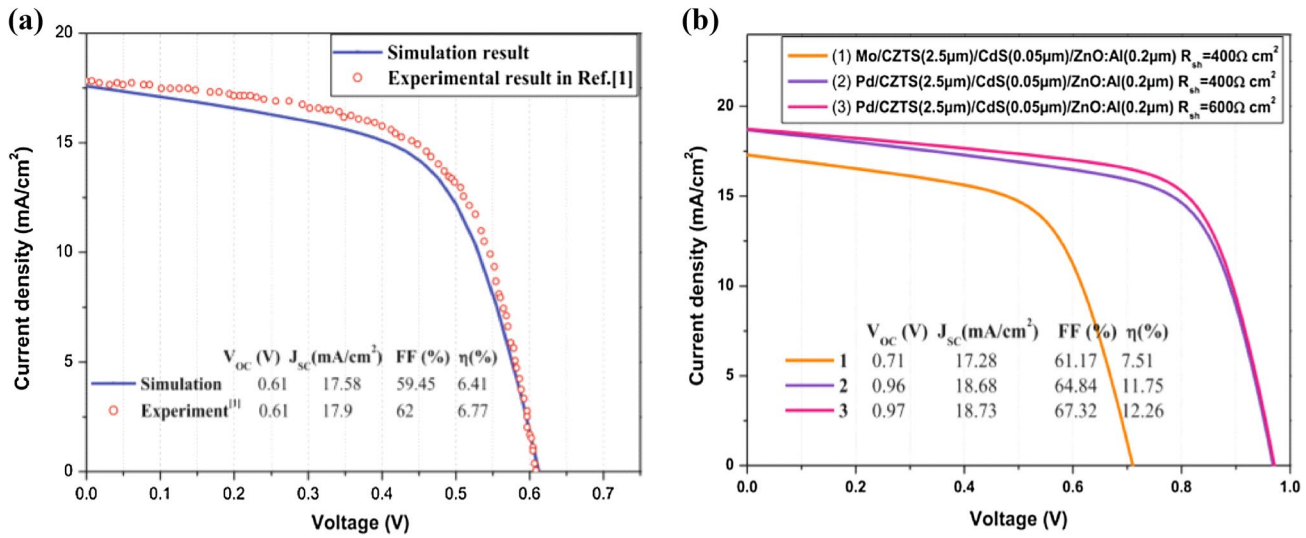

Fig. 12 J–V characteristics of CZTS solar cells **a** experiment [25] and observation **b** optimized [89]

Table 9 Cell parameters obtained from simulations with three sets of CZTS (n,k) values, compared to experimental data

Device with various optical constants	η (%)	J_{SC} (mA/cm^2)	V_{OC} (V)	FF (%)
Experimental [31]	8.4	19.5	0.66	65.8
Sim_nk_Theory [106]	4.68	10.79	0.63	68
Sim_nk_bulk [106]	8.78	20.79	0.66	63
Sim_nk_fit [106]	8.24	19.40	0.65	65

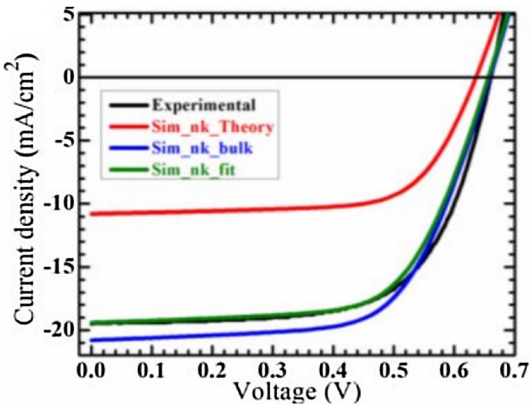

Fig. 13 J–V characteristics from simulation with *n, k* values obtained from calculations (Sim_nk_Theory), bulk measurement (Sim_nk_bulk) and fitting (Sim_nk_fit) [106], with the experimental data [31] shown for comparison

cell with carrier concentration gradient of CZTS, small spike-like CBO of 0.1 eV for $\chi_{CZTS} = 4.3$ eV and p-MoS_2 between CZTS/Mo interface.

Table 10 Output performance of the numerical simulation Kesterite solar cell by different softwares

Software	η (%)	J_{SC} (mA/cm^2)	V_{OC} (V)	FF (%)	References
AZO/CdS/CZTS/Mo					
SCAPS-1D	12.26	18.73	0.97	67.32	[89]
	13.41	19.31	1.002	69.35	[96]
	18.05	25.67	1.02	69.26	[99]
AMPS-1D	15.68	19.99	0.956	82.1	[107]
AZO/i-ZnO/CdS/CZTS/Mo					
SCAPS	14.57	18.68	1.009	77.29	[98]
ATLAS	8.51	19.18	0.692	64.1	[94]
Sentaurus	8.78	20.79	0.665	63	[106]

Many issues were resulted by this numerical model, and also permit became easy to understand CZTS thin-films solar cell with natural complex structure. Additional investigation is needed, though, to reinforce the understanding of long-term material stability, as well as to help advance this new technology.

Acknowledgements The authors gratefully acknowledge anonymous reviewers for their scientific suggestions and constructive comments.

References

1. M.A. Green et al., Solar cell efficiency tables (version 50). Prog. Photovolt. Res. Appl. **25**(7), 668–676 (2017)
2. M. Jiang, X. Yan, Cu2ZnSnS4 thin film solar cells: present status and future prospects. In *Solar Cells—Research and Application Perspectives*, (InTech, UK, 2013)
3. H. Katagiri, N. Sasaguchi, S. Hando, S. Hoshino, J. Ohashi, T. Yokota, Preparation and evaluation of Cu2ZnSnS4 thin films

by sulfurization of EB evaporated precursors. Sol. Energy Mater. Sol. Cells **49**(1), 407–414 (1997)
4. H. Katagiri, N. Ishigaki, T. Ishida, K. Saito, Characterization of CuZnSnS thin films prepared by vapor phase sulfurization. Jpn. J. Appl. Phys. **40**, 500–504 (2001)
5. T. Tanaka et al., Preparation of Cu2ZnSnS4 thin films by hybrid sputtering. J. Phys. Chem. Solids **66**(11), 1978–1981 (2005)
6. J. Zhang, L. Shao, Y. Fu, E. Xie, Cu2ZnSnS4 thin films prepared by sulfurization of ion beam sputtered precursor and their electrical and optical properties. Rare Met. **25**, 315–319 (2006)
7. N. Kamoun, H. Bouzouita, B. Rezig, Fabrication and characterization of Cu2ZnSnS4 thin films deposited by spray pyrolysis technique. Thin Solid Films **515**(15), 5949–5952 (2007)
8. J.J. Scragg, P.J. Dale, L.M. Peter, G. Zoppi, I. Forbes, New routes to sustainable photovoltaics: evaluation of Cu_2ZnSnS_4 as an alternative absorber material, Phys. Status Solidi B **245**(9), 1772–1778 (2008)
9. P.A. Fernandes, P.M.P. Salomé, A.F. da Cunha, Precursors order effect on the properties of sulfurized Cu $_2$ZnSnS_4 thin films. Semicond. Sci. Technol. **24**(10), 105013 (2009)
10. C.P. Chan, H. Lam, C. Surya, Preparation of Cu2ZnSnS4 films by electrodeposition using ionic liquids. Sol. Energy Mater. Sol. Cells **94**(2), 207–211 (2010)
11. J.P. Leitão et al., Study of optical and structural properties of Cu2ZnSnS4 thin films. Thin Solid Films **519**(21), 7390–7393 (2011)
12. Z. Su et al., Preparation of Cu2ZnSnS4 thin films by sulfurizing stacked precursor thin films via successive ionic layer adsorption and reaction method. Appl. Surf. Sci. **258**(19), 7678–7682 (2012)
13. N.M. Shinde, R.J. Deokate, C.D. Lokhande, Properties of spray deposited Cu2ZnSnS4 (CZTS) thin films. J. Anal. Appl. Pyrolysis **100**, 12–16 (2013)
14. M.Z. Ansari, N. Khare, Structural and optical properties of CZTS thin films deposited by ultrasonically assisted chemical vapour deposition. J. Phys. Appl. Phys. **47**(18), 185101 (2014)
15. R. Touati, M. Ben Rabeh, M. Kanzari, 'Effect of post-sulfurization on the structural and optical properties of Cu 2 ZnSnS4 thin films deposited by vacuum evaporation method'. Thin Solid Films **582**, 198–202 (2015)
16. F. Aslan, A. Göktaş, A. Tumbul, Influence of pH on structural, optical and electrical properties of solution processed Cu2ZnSnS4 thin film absorbers. Mater. Sci. Semicond. Process. **43**, 139–143 (2016)
17. M. Courel, J.A. Andrade-Arvizu, A. Guillén-Cervantes, M.M. Nicolás-Marín, F.A. Pulgarín-Agudelo, O. Vigil-Galán, Optimization of physical properties of spray-deposited Cu 2 ZnSnS 4 thin films for solar cell applications. Mater. Des. **114**, 515–520 (2017)
18. A. Tumbul, M.Z. Göktaş, Zarbali, F. Aslan, Structural, morphological and optical properties of the vacuum-free processed CZTS thin film absorbers. Mater. Res. Express **5**(6), 066408 (2018)
19. Yan et al., Cu2ZnSnS4 solar cells with over 10% power conversion efficiency enabled by heterojunction heat treatment. Nat. Energy **3**(9), 764–772 (2018)
20. K. Sun et al., Over 9% efficient kesterite Cu_2ZnSnS_4 solar cell fabricated by using $Zn_{1-x}Cd_x$ S buffer layer. Adv. Energy Mater. **6**(12), 1600046 (2016)
21. H. Katagiri, K. Saitoh, T. Washio, H. Shinohara, T. Kurumadani, S. Miyajima, Development of thin film solar cell based on Cu2ZnSnS4 thin films. Sol. Energy Mater. Sol. Cells **65**, 141–148 (2001)
22. H. Katagiri, K. Jimbo, K. Moriya, K. Tsuchida, Solar cell without environmental pollution by using CZTS thin film. In *Proceedings of 3rd World Conference on Photovoltaic Energy Conversion*, vol. 3 (IEEE, 2003), pp. 2874–2879
23. T. Kobayashi, K. Jimbo, K. Tsuchida, S. Shinoda, T. Oyanagi, H. Katagiri, Investigation of Cu ZnSnS-based thin film solar cells using abundant materials. Jpn. J. Appl. Phys. **44**, 783–787 (2005)
24. K. Moriya, K. Tanaka, H. Uchiki, Fabrication of CuZnSnS thin-film solar cell prepared by pulsed laser deposition. Jpn. J. Appl. Phys. **46**, 5780–5781 (2007)
25. H. Katagiri et al., Enhanced conversion efficiencies of CuZnSnS -based thin film solar cells by using preferential etching technique. Appl. Phys. Express **1**, 041201 (2008)
26. A. Ennaoui et al., Cu2ZnSnS4 thin film solar cells from electroplated precursors: Novel low-cost perspective. Thin Solid Films **517**(7), 2511–2514 (2009)
27. K. Wang et al., Thermally evaporated Cu2ZnSnS4 solar cells. Appl. Phys. Lett. **97**(14), 143508 (2010)
28. K. Tanaka, Y. Fukui, N. Moritake, H. Uchiki, Chemical composition dependence of morphological and optical properties of Cu2ZnSnS4 thin films deposited by sol–gel sulfurization and Cu2ZnSnS4 thin film solar cell efficiency. Sol. Energy Mater. Sol. Cells **95**(3), 838–842 (2011)
29. K. Maeda, K. Tanaka, Y. Fukui, H. Uchiki, Influence of H2S concentration on the properties of Cu2ZnSnS4 thin films and solar cells prepared by sol–gel sulfurization. Sol. Energy Mater. Sol. Cells **95**(10), 2855–2860 (2011)
30. R.B.V. Chalapathy, G.S. Jung, B.T. Ahn, Fabrication of Cu2ZnSnS4 films by sulfurization of Cu/ZnSn/Cu precursor layers in sulfur atmosphere for solar cells. Sol. Energy Mater. Sol. Cells **95**(12), 3216–3221 (2011)
31. B. Shin, O. Gunawan, Y. Zhu, N.A. Bojarczuk, S.J. Chey, S. Guha, 'Thin film solar cell with 8.4% power conversion efficiency using an earth-abundant Cu_2ZnSnS_4 absorber: Cu_2ZnSnS_4 solar cell with 8.4% efficiency'. Prog. Photovolt. Res. Appl. **21**(1), 72–76 (2013)
32. S. Ahmed, K.B. Reuter, O. Gunawan, L. Guo, L.T. Romankiw, H. Deligianni, A high efficiency electrodeposited Cu2ZnSnS4 solar cell. Adv. Energy Mater. **2**(2), 253–259 (2012)
33. T. Fukano, S. Tajima, T. Ito, Enhancement of conversion efficiency of CuZnSnS thin film solar cells by improvement of sulfurization conditions. Appl. Phys. Express, **6**, 062301 (2013)
34. P. Emrani, Vasekar, C.R. Westgate, Effects of sulfurization temperature on CZTS thin film solar cell performances. Sol. Energy **98**, 335–340 (2013)
35. T.P. Dhakal, C. Peng, R. Reid Tobias, R. Dasharathy, C.R. Westgate, Characterization of a CZTS thin film solar cell grown by sputtering method. Sol. Energy **100**, 23–30 (2014)
36. F. Jiang, S. Ikeda, T. Harada, M. Matsumura, Pure sulfide Cu_2ZnSnS_4 thin film solar cells fabricated by preheating an electrodeposited metallic stack. Adv. Energy Mater. **4**(7), 1301381 (2014)
37. J. Tao et al., A sputtered CdS buffer layer for co-electrodeposited CuZnSnS solar cells with 6.6% efficiency. Chem. Commun. **51**, 10337–10340 (2015)
38. J. Tao et al., 7.1% efficient co-electroplated CuZnSnS thin film solar cells with sputtered CdS buffer layers. Green Chem. **18**, 550–557 (2016)
39. S. Tajima, M. Umehara, M. Hasegawa, T. Mise, T. Itoh, Cu $_2$ZnSnS_4 photovoltaic cell with improved efficiency fabricated by high-temperature annealing after CdS buffer-layer deposition: Cu $_2$ZnSnS_4 photovoltaic cell with improved efficiency. Prog. Photovolt. Res. Appl. **25**(1), 14–22 (2017)
40. M.G. Sousa, A.F. da Cunha, J.P. Teixeira, J.P. Leitão, G. Otero-Irurueta, M.K. Singh, Optimization of post-deposition annealing in Cu 2 ZnSnS 4 thin film solar cells and its impact on device performance. Sol. Energy Mater. Sol. Cells **170**, 287–294 (2017)
41. S. Rühle, Tabulated values of the Shockley–Queisser limit for single junction solar cells. Sol. Energy **130**, 139–147 (2016)

42. M. Mazzeret al., Bifacial CIGS solar cells grown by low temperature pulsed electron deposition. Sol. Energy Mater. Sol. Cells **166**, 247–253 (2017)
43. P. Jackson, R. Wuerz, D. Hariskos, E. Lotter, W. Witte, M. Powalla, 'Effects of heavy alkali elements in Cu(In,Ga)Se_2 solar cells with efficiencies up to 22.6%'. Phys. Status Solidi RRL Rapid Res. Lett. **10**(8), 583–586 (2016)
44. K. Zhang, H. Guo, Effects of annealing on Cu2ZnSnS4 thin films prepared on Mo substrate and the fabrication of solar cells. J. Mater. Sci. Mater. Electron. **28**(22), 17044–17048 (2017)
45. J. Tao et al., Co-electrodeposited CuZnSnS thin-film solar cells with over 7% efficiency fabricated via fine-tuning of the Zn content in absorber layers. J. Mater. Chem. A **4**, 3798–3805 (2016)
46. N. Naghavi et al., Buffer layers and transparent conducting oxides for chalcopyrite Cu(In,Ga)(S,Se)2 based thin film photovoltaics: present status and current developments. Prog. Photovolt. Res. Appl. **18**(6), 411–433 (2010)
47. M. Polman, E.C. Knight, B. Garnett, Ehrler, W.C. Sinke, Photovoltaic materials: present efficiencies and future challenges. Science **352**(6283), aad4424 (2016)
48. H. Katagiri, K. Jimbo, M. Tahara, H. Araki, K. Oishi, The influence of the composition ratio on CZTS-based thin film solar cells., MRS Proc. **1165**, (2009)
49. M.T. Htay et al., A cadmium-free Cu_2ZnSnS_4/ZnO hetrojunction solar cell prepared by practicable processes. Jpn. J. Appl. Phys. **50**, 032301 (2011)
50. A.I. Inamdar, K.-Y. Jeon, H. Woo, W. Jung, H. Im, H. Kim, Synthesis of a Cu2ZnSnS4 (CZTS) absorber layer and metal doped ZnS buffer layer for heterojunction solar cell applications. ECS Trans. **41**(4), 167–175 (2011)
51. J. Kim et al., Optimization of sputtered ZnS buffer for Cu2ZnSnS4 thin film solar cells. Thin Solid Films **566**, 88–92 (2014)
52. V.G. Rajeshmon, C.S. Kartha, K.P. Vijayakumar, A.B. Garg, R. Mittal, R. Mukhopadhyay, Spray pyrolysed Cu[sub 2]ZnSnS[sub 4] solar cell using cadmium free buffer layer', presented at the solid state physics, proceedings of the 55th day solid state physics symposium 2010 (Manipal, 2011) pp. 683–684
53. J. Yu et al., Effect of deposited temperatures of the buffer layer on the band offset of CZTS/In $_2$ S $_3$heterostructure and its solar cell performance. Chin. Phys. B **26**(4), 046802 (2017)
54. T. Ericson et al., Zn(O, S) Buffer layers and thickness variations of CdS buffer for Cu $_{2}$ZnSnS$_{4}$ solar cells. IEEE J. Photovolt. **4**(1), 465–469 (2014)
55. C. Platzer-Björkman et al., Reduced interface recombination in Cu_2ZnSnS_4 solar cells with atomic layer deposition $Zn_{1-x}Sn_xO_y$ buffer layers. Appl. Phys. Lett. **107**(24), 243904 (2015)
56. T. Ericson et al., Zinc–Tin–Oxide buffer layer and low temperature post annealing resulting in a 9.0% efficient Cd-free Cu $_2$ZnSnS$_4$ solar cell. Sol. RRL **1**(5), 1700001 (2017)
57. X. Cui et al., Enhanced heterojunction interface quality to achieve 9.3% efficient Cd-free Cu $_2$ZnSnS$_4$ solar cells using atomic layer deposition ZnSnO buffer layer. Chem. Mater. **30**(21), 7860–7871 (2018)
58. W. Wang et al., The effects of SnS $_2$ secondary phases on Cu $_2$ZnSnS$_4$ solar cells: a promising mechanical exfoliation method for its removal. J. Mater. Chem. A **6**(7), 2995–3004 (2018)
59. T.J. Huang, X. Yin, G. Qi, H. Gong, CZTS-based materials and interfaces and their effects on the performance of thin film solar cells: CZTS-based materials and interfaces and their effects on the performance of thin film solar cells. Phys. Status Solidi RRL **08**(09), 735–762 (2014)
60. D. Mamedov, M. Klopov, S.Z. Karazhanov, Influence of Cu2S, SnS and Cu2ZnSnSe4 on optical properties of Cu2ZnSnS4. Mater. Lett. **202**, 70–72 (2017)
61. T. Gokmen, O. Gunawan, T.K. Todorov, D.B. Mitzi, Band tailing and efficiency limitation in kesterite solar cells. Appl. Phys. Lett. **103**(10), 103506 (2013)
62. C. Yan, J. Huang, K. Sun, Y. Zhang, M.A. Green, X. Hao, Efficiency improvement of high band gap Cu2ZnSnS4 solar cell achieved by silver incorporation. In *IEEE 7th World Conference on Photovoltaic Energy Conversion (WCPEC) (A Joint Conference of 45th IEEE PVSC, 28th PVSEC & 34th EU PVSEC)*, pp. 3709–3711 (2018)
63. C.-Y. Liu, Z.-M. Li, H.-Y. Gu, S.-Y. Chen, H. Xiang, X.-G. Gong, Sodium passivation of the grain boundaries in $CuInSe_2$ and Cu $_2$ZnSnS$_4$ for high-efficiency solar cells. Adv. Energy Mater. **7**(8), 1601457 (2017)
64. S. Zhuk, A. Kushwaha, T.K.S. Wong, S. Masudy-Panah, A. Smirnov, G.K. Dalapati, 'Critical review on sputter-deposited Cu2ZnSnS4 (CZTS) based thin film photovoltaic technology focusing on device architecture and absorber quality on the solar cells performance'. Sol. Energy Mater. Sol. Cells **171**, 239–252 (2017)
65. M. Courel, E. Valencia-Resendiz, J.A. Andrade-Arvizu, E. Saucedo, O. Vigil-Galán, 'Towards understanding poor performances in spray-deposited Cu 2 ZnSnS 4 thin film solar cells. Sol. Energy Mater. Sol. Cells **159**, 151–158 (2017)
66. M. Courel et al., Study on the impact of stoichiometric and optimal compositional ratios on physical properties of Cu $_2$ZnSnS$_4$ thin films deposited by spray pyrolysis. Mater. Res. Express **5**(1), 015513 (2018)
67. C.W. Hong, S.W. Shin, M.P. Suryawanshi, M.G. Gang, J. Heo, J.H. Kim, Chemically deposited CdS buffer/kesterite Cu $_2$ZnSnS$_4$ solar cells: relationship between CdS thickness and device performance. ACS Appl. Mater. Interfaces **9**(42), 36733–36744 (2017)
68. S. Rondiya et al., CZTS/CdS: interface properties and band alignment study towards photovoltaic applications. J. Mater. Sci. Mater. Electron. **29**(5), 4201–4210 (2018)
69. F. Liu et al., Enhancing the Cu_2ZnSnS_4 solar cell efficiency by back contact modification: Inserting a thin TiB_2 intermediate layer at Cu_2ZnSnS_4/Mo interface. Appl. Phys. Lett. **104**(5), 051105 (2014)
70. H. Cui et al., Improvement of Mo/Cu2ZnSnS4 interface for Cu2ZnSnS4 (CZTS) thin film solar cell application. MRS Proc., 1638 (2014)
71. W. Li, J. Chen, H. Cui, F. Liu, X. Hao, Inhibiting MoS2 formation by introducing a ZnO intermediate layer for Cu2ZnSnS4 solar cells. Mater. Lett. 130, 87–90 (2014)
72. Z. Wei et al., Engineering of a Mo/Si_xN_y diffusion barrier to reduce the formation of MoS_2 in Cu_2ZnSnS_4 thin film solar cells. ACS Appl. Energy Mater. **1**(6), 2749–2757 (2018)
73. J. Park et al., 'The effect of thermal evaporated MoO_3 intermediate layer as primary back contact for kesterite Cu 2 ZnSnS 4 solar cells. Thin Solid Films **648**, 39–45 (2018)
74. S. Selberherr, *Analysis and simulation of semiconductor devices* (Springer, New York, 2013)
75. J.L. Gray, ADEPT: a general purpose numerical device simulator for modeling solar cells in one-, two-, and three-dimensions, In *Photovoltaic Specialists Conference, Conference Record of the Twenty Second IEEE*, pp. 436–438 (1991)
76. S.J. Fonash et al., A manual for AMPS-1D: a one-dimensional device simulation program for the analysis of microelectronic and photonic structures, Pennsylvania State University
77. R. Stanglet al., 'AFORS-HET a numerical PC-program for simulation of heterojunction solar, cells, version 1.1 (open-source on demand), to be distributed for public use. In *Proc. 19th PVSEC, Paris, France*, p. 1497 (2004)
78. 'Semiconductor Software, Modeling the physics of semiconductor devices. https://www.comsol.fr/semiconductor-module. Accessed: 30 Sep 2018 **(Online)**

79. PC1Dmod User Manual 6.1, Institute for Energy Technology, Norway & Fraunhofer Institute for Solar Energy Systems, Germany. https://www2.pvlighthouse.com.au/resources/PC1D/PC1Dmod6/PC1Dmod%206-1%20help.pdf. Accessed 21 Jan 2019
80. M. Burgelman et al., SCAPS manual, University of Gent, Belgium (2018)
81. SILVACO International, ATLAS user's manual: device simulation software (2004)
82. D.M. Caughey, R.E. Thomas, Carrier mobilities in silicon empirically related to doping and field. Proc. IEEE **55**, 2192–2193 (1967)
83. N.D. Arora, J.R. Hauser, D.J. Roulston, Electron and hole mobilities in silicon as a function of concentration and temperature. IEEE Trans. Electron Devices **29**, 292–295 (1982)
84. J.M. Dorkel, P. Leturcq, Carrier mobilities in silicon semi-empirically related to temperature, doping and injection level. Solid State Electron. **24**(9), 821–825 (1981)
85. D.B.M. Klaassen, A unified mobility model for device simulation, In *International Technical Digest on Electron Devices, San Francisco, CA, USA, 1990*, pp. 357–360 (1990)
86. M. Burgelman, J. Verschraegen, S. Degrave, P. Nollet, Modeling thin-film PV devices. Prog. Photovolt. Res. Appl. **12**(23), 143–153 (2004)
87. A. Haddout, A. Raidou, M. Fahoume, Numerical modeling of CdTe solar cells thin film investigation by using PC1D model. World J. Eng. **15**, 549–555 (2018)
88. A. Haddout, Raidou, M. Fahoume, Influence of the layer parameters on the performance of the CdTe solar cells. Optoelectron. Lett. **14**(2), 98–103 (2018)
89. A. Haddout, M. Raidou, N. Fahoume, Elharfaoui, M. Lharch, Influence of CZTS layer parameters on cell performance of Kesterite thin-film solar cells. In *Proceedings of the 1st International Conference on Electronic Engineering and Renewable Energy*, vol. 519, ed. by B. Hajji, G.M. Tina, K. Ghoumid, A. Rabhi, A. Mellit (Springer, Singapore, 2019), pp. 640–646
90. T. Frisk, S.-Y. Ericson, P. Li, J. Szaniawski, Olsson, C. Platzer-Björkman, Combining strong interface recombination with bandgap narrowing and short diffusion length in Cu 2 ZnSnS 4 device modeling. Sol. Energy Mater. Sol. Cells **144**, 364–370 (2016)
91. A. Pu et al., Sentaurus modelling of 6.9% Cu 2 ZnSnS 4 device based on comprehensive electrical & optical characterization. Sol. Energy Mater. Sol. Cells **160**, 372–381 (2017)
92. L.-Y. Lin, Y. Qiu, Y. Zhang, H. Zhang, Analysis of Effect of Zn(O,S) Buffer Layer Properties on CZTS Solar Cell Performance Using AMPS. Chin. Phys. Lett. **33**(10), 107801 (2016)
93. M. Jani, D. Raval, I. Mukhopadhyay, A. Ray, Reinforcement of Zn(O,S) buffer layer for efficient band matching in a kesterite (Cu2ZnSnS4) solar cell and its analysis using simulation tool for the application in energy harvesting. In *Presented at the Functional Oxides And Nanomaterials: Proceedings of the International Conference on Functional Oxides and Nanomaterials*, vol. 1837, p. 040060 (2017)
94. V. Sivathanu, T. Rajalingam, T.R. Lenka, Modelling of CZTS/ZnS/AZO solar cell for efficiency enhancement. In *2018 3rd International Conference on Microwave and Photonics (ICMAP)*, IEEE, pp. 1–2 (2018)
95. M. Bahfir, Boumaour, M. Kechouane, Prospects of potential ZnMgO front layer in CZTS solar cells. Optik **169**, 196–202 (2018)
96. M. Patel, A. Ray, Enhancement of output performance of Cu2ZnSnS4 thin film solar cells—A numerical simulation approach and comparison to experiments. Phys. B Condens. Matter **407**(21), 4391–4397 (2012)
97. J. Xu, Investigation of Cu2ZnSnS4 thin-film solar cells with carrier concentration gradient. J. Phys. Chem. Solids **98**, 32–37 (2016)
98. S.R. Meher, L. Balakrishnan, Z.C. Alex, Analysis of Cu2ZnSnS4/CdS based photovoltaic cell: A numerical simulation approach. Superlattices Microstruct. **100**, 703–722 (2016)
99. D. Adewoyin, M.A. Olopade, M. Chendo, Enhancement of the conversion efficiency of Cu2ZnSnS4 thin film solar cell through the optimization of some device parameters. Opt. Int. J. Light Electron Opt. **133**, 122–131 (2017)
100. Y.H. Khattak, F. Baig, S. Ullah, B. Marí, S. Beg, H. Ullah, Enhancement of the conversion efficiency of thin film kesterite solar cell. J. Renew. Sustain. Energy **10**(3), 033501 (2018)
101. Kumar, A.D. Thakur, Role of contact work function, back surface field, and conduction band offset in Cu_2ZnSnS_4 solar cell. Jpn. J. Appl. Phys. **57**(8S3), 08RC05 (2018)
102. W. Zhao, W. Zhou, X. Miao, Numerical simulation of CZTS thin film solar cell. In *7th IEEE International Conference on Nano/Micro Engineered and Molecular Systems (NEMS)*, pp. 502–505 (2012)
103. K. Wang, B. Shin, K.B. Reuter, T. Todorov, D.B. Mitzi, S. Guha, Structural and elemental characterization of high efficiency Cu2ZnSnS4 solar cells. Appl. Phys. Lett. **98**(5), 051912 (2011)
104. P. Chelvanathan, M.I. Hossain, J. Husna, M. Alghoul, K. Sopian, N. Amin, Effects of transition metal dichalcogenide molybdenum disulfide layer formation in Copper–Zinc–Tin–Sulfur solar cells from numerical analysis. Jpn. J. Appl. Phys. **51**, 10NC32 (2012)
105. M.T. Ferdaous et al., Elucidating the role of interfacial MoS2 layer in Cu2ZnSnS4 thin film solar cells by numerical analysis. Sol. Energy **178**, 162–172 (2019)
106. S.M. Mopurisetty, M. Bajaj, S. Ganguly, TCAD calibration for Cu2ZnSnS4 solar cell simulation, In *2016 IEEE 43rd, Photovoltaic Specialists Conference (PVSC)*, pp. 2228–2231 (2016)
107. J.H.N. Tchognia et al., Optimization of the output parameters in kesterite-based solar cells by AMPS-1D, In *2015 3rd International, Renewable and Sustainable Energy Conference (IRSEC)*, IEEE, pp. 1–6 (2015)